ANALYSIS OF TEMPERATURE AND THERMAL INERTIA OF THE SURFACE OF VESTA USING DAWN VIR SURVEY OBSERVATIONS.

T.N. Titus[1], K. Becker[1], F. Tosi[2], M.T. Capria[2], M.C. De Sanctis[2], E. Palomba[2], D. Grassi[2], F. Capaccioni[2], E. Ammannito[2], J.-Ph. Combe[3], T.B. McCord[3], J.-Y. Li[4], C.T. Russell[5], C.A. Raymond[6], [1]Astrogeology Science Center, U.S. Geological Survey. [2]INAF-IAPS (Istituto di Astrofisica e Planetologia Spaziali),. [3]Bear Fight Institute,. [4]Planetary Science Institute, [5]Institute of Geophysics and Planetary Physics, University of California at Los Angeles, [6]Jet Propulsion Laboratory, California Institute of Technology.

Introduction: In this work, we compare observed temperatures of the surface of Vesta using data acquired by the Dawn [1] Visible and Infrared mapping spectrometer (VIR) [2] during Survey phase to model results using the KRC thermal model [3].

Thermal Inertia: Thermal inertia (I) is a measure of how quickly a material's temperature responds to changes in energy input, and is defined as $I=\sqrt{k\rho c}$, where k is the thermal conductivity, ρ is the bulk density, and c is the specific heat capacity. SI units for I are J m^{-2} $s^{-1/2}$ K^{-1} , henceforth referred to as ''TIU'' (thermal inertia unit) as proposed by Putzig [4].

High thermal-inertia materials, such as bedrock, resist changes in temperature while temperatures of low thermal inertia materials, such as dust, respond quickly to changes in solar insolation. The surface of Vesta is expected to have low-to-medium thermal inertia values, with the most commonly used value being extremely low at 15 TIU [e.g. 5].

There are several parameters that affect observed temperatures in addition to thermal inertia, e.g. Bond albedo, slope, and surface roughness. In addition to these parameters, real surfaces are rarely uniform monoliths that can be described by a single thermal inertia value. Real surfaces are often vertically layered mixtures of dust and rock. For Vesta's surface, with temperature extremes ranging from 50 K to 275 K [5] and no atmosphere, even a uniform monolithic surface may have non-uniform thermal inertia due to temperature-dependent thermal conductivity.

Data: The Dawn spacecraft [1] acquired survey observations (mean orbital altitude ~2,700 km) from 11 to 31 August 2011. **Fig. 1** shows a non-map projected false-color view of Vesta as seen by VIR in the near-infrared.

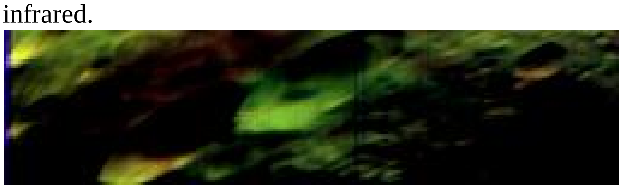

Figure 1: Dawn VIR IR False Color Unprojected Image (VIR_IR_1B_1_364718678_1).where RGB is 4μm, 3 μm, 2μm, respectively.

Temperature Calculations: Surface temperatures were calculated from VIR spectral radiance data at infrared wavelengths longward of 4 μm using a Bayesian approach to nonlinear inversion as described by Tosi et al. [6, 7]. **Fig. 2** is an example of the derived surface temperatures.

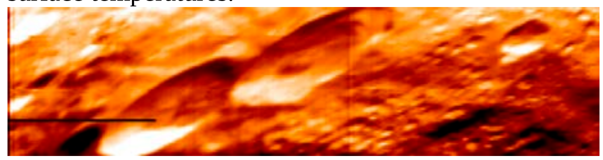

Figure 2: Surface temperatures derived from VIR infrared data for the same hyperspectral image of Fig. 1. Black corresponds to the minimum temepratureof 208 K and white corresponds to the maximum temperature of 261 K.

Other model input parameters: In order to compare observed temperatures of Vesta with modeled values, several geometric and photometric parameters must be known or estimated. These include local mean solar time, latitude, local slope, bond bolometric albedo, and the effective emissivity at 5 μm. Local time, latitude, and local slope are calculated using the USGS ISIS software system [8, 9]. The bolometric bond albedo is estimated from a normalized photometrically-corrected Dawn Framing Camera mosaic (see **Fig. 3**) that assumes the darkest regions of Vesta are consistent with a Bond albedo of 0.1 and that the brightest regions are consistent with a Bond albedo of 0.35.

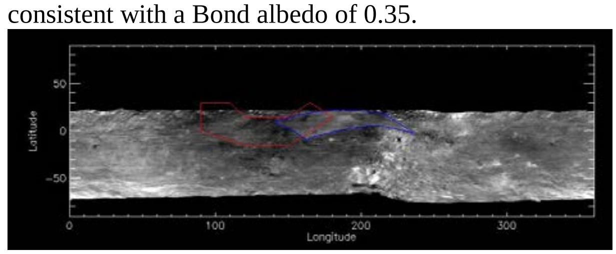

Figure 3: Photometrically-corrected normalized FC Mosaic. Red outlines a region of enhanced hydrogen detection by GRaND. Blue outlines the location of VIR image VIR_IR_1B_1_364718678_1.

Models: We employ a multi-layered thermal-diffusion model called 'KRC' [5], which has been used extensively in the study of Martian thermophysical properties [e.g. 5,6]. This thermal model is easily modified for use with Vesta by replacing the Martian ephemeris input with the Vesta ephemeris and turning the atmosphere off. This model calculates surface temperatures throughout an entire Vesta year for a specific set of slope, azimuth, latitude, elevation and albedo for up to ten different thermal inertia values. To calculate surface temperatures, KRC uses the Delta-Eddington approximation for radiative flux [5] to solve the subsurface thermal diffusion equation using finite-difference methods. The upper boundary condition is insolation (calculated at each step according to orbital position, orbital inclination and time of day). KRC was executed several times in order to build a suite of models (8 dimensional look up table) that spans the parameter space that determines the surface temperature of Vesta. The range of parameters is listed in **Table 1**.

Table 1: KRC Model Suite Parameters.

Parameter	Min	Max	Interval	Units
Season	0	360		
Latitude	-80	80	20	Degrees
Local Time	0	24	1	Hours
Thermal Inertia	11	42	Sqrt(2)	TIU (SI Units)
Slope dz/dx	0	45	~11	Degrees
Slope dz/dy	0	45	~11	Degrees
Albedo	0	.3	0.05	
Emissivity	0.1	1.0	0.1	

Table 2: Sources used to constrain model parameters.

Parameter	Source	Min	Max
Season	PDS Header		
Local Time	ISIS3	11	13
Latitude	ISIS3	80S	80N
Slopes	ISIS3 Gaskell Shape Model	0	45
Bond Albedo	J-Y Li Normized FC Mosaic (Fig. 2)	0.1	0.35

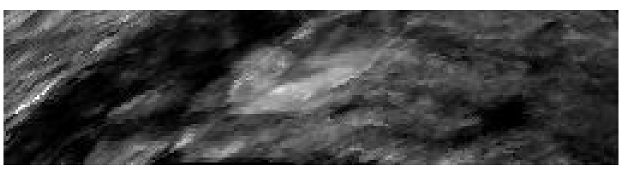

Figure 4: Estimated Bond Albedo derived from Normalized FC mosaic.

Figure 5: Slopes derived from the Gaskell shape model. Slopes range from 0 (black) to 40.2º (white).

Processing: The 8-dimensional lookup-table KRC models are run with varying values for albedo, thermal inertia and layer depth to create temperature indices which are closely matched, via bilinear interpolation, to the dates and times observed by VIR. After this interpolation, our working index contains modeled temperatures for all times of observation at a logarithmic range of five thermal inertias between 11 and 42 TIU. Higher values of TIU can be included if necessary. The downhill-simplex method of function minimization is then applied to compare the observed and modeled temperatures to determine a single best-fit value for thermal inertia and effective emissivity for the VIR scene (or image). Since the simultaneous determination of both effective emissivity and thermal inertia is non-unique, we initially assume that the effective emissivity for a given pixel is that same as the best-fit emissivity for the entire scene. The thermal inertia that has the same model temperature as observed is then selected.

Results: In this analysis, we attempted to remove many of the surface physical properties that influence variations in thermal emission, especially effects from slopes, latitude, local time of day and albedo. For the VIR data shown in **Figs. 6-8**, it is clear that not all topographical (and perhaps albedo) effects have been completely removed. Still, there are indications of patches of unusually high and low thermal inertia that merit further investigation.

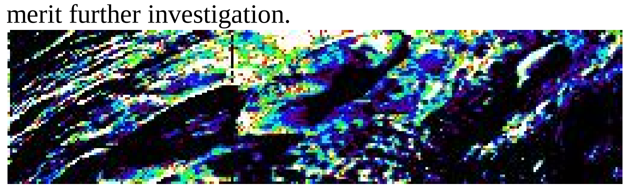

Figure 6: Colorized Thermal Inertia ranging from 11 TIU (black) to 42 TUI (white).

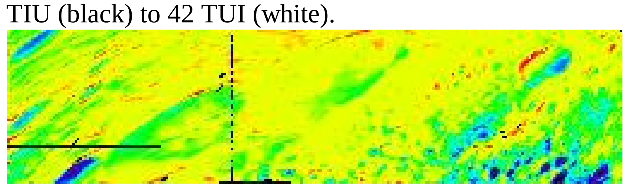

Figure 7: Colorized Effective Emissivity ranging from 0.1 (black) to 1.0 (red-white).

Acknowledgements: The authors gratefully acknowledge the support of the Dawn Instrument Operations, and Science Teams. This work is supported by an Italian Space Agency (ASI) grant and by NASA through the Dawn project and the Dawn at Vesta Participating Scientists program.

References: [1] C.T. Russell, et al., Planetary and Space Science, 52, 465–489, 2004. [2] De Sanctis, M.C., et al. (2010). *Space Sci. Rev.*, doi: 10.1007/s11214-010-9668-5. [3] Kieffer et al., (1977) *JGR*, *82*, 4249-4291. [4] N. E. Putzig (2006) Ph.D. Dissertation. [5] Spencer (1990) Icarus, 83, 27- 38. [6] Tosi, F., et al. (2012) In preparation. [7] F. Tosi et al. (2012) *LPS XLIII* [8] Anderson, J. A., et al. (2004), *LPSC XXXV*, abstract 2039 [9] K. Becker et al. (2012) *LPS XLIII*. [6] Titus et al. (2003) *Sci.*, *299*, 1048-1051.